

# A Discussion on Major Factors Affecting Crack Path of Concrete-to-Concrete Interfacial Surfaces

A. Satoh<sup>1</sup>, K. Yamada<sup>2</sup> and S. Ishiyama<sup>3</sup>

<sup>1, 2 and 3</sup> Akita Prefectural University, Tsuchiya, Yurihonjo, Akita, 015-0055, Japan;  
<sup>1</sup>m09c003@akita-pu.ac.jp, <sup>2</sup>kanji\_yamada@akita-pu.ac.jp, <sup>3</sup>ishiyama@akita-pu.ac.jp

**ABSTRACT.** *This paper elaborates major factors which affect the crack path of concrete-to-concrete interfacial surfaces produced with placing joint. Specimens with eight types of placing joints and three types of monolithic ones were employed for the evaluation of tension softening diagram followed by surface observations of the ligament after fracture test. The SEM and EPMA analysis revealed that the layer of Ca(OH)<sub>2</sub> plays a primary role on the crack path, which was clearly detected by a map that indicates Ca/Si ratio. The ratio of fractured part excluding detached part on the surface divided by the total ligament area was defined as  $\Phi$ , which proved to be an important value which is related to initial closure stress ( $f_i$ ) and also the maximum height on the fractured surface ( $P_t$ ). As both  $f_i$  and  $P_t$  affect strength (bending strength  $f_b$ ) and ductility in terms of fracture energy ( $GF$ ), both  $f_b$  and  $GF$  are affected by  $\Phi$ . Then the most important treatment for the better mechanical performance for the interface is removing Ca(OH)<sub>2</sub> and obtains large  $\Phi$ .*

## INTRODUCTION

Every concrete structure has inevitably concrete-to-concrete interfacial surfaces such as construction joint, casting of additional concrete for reinforcement and laying of cover layer for the finishing. In these days of heading towards rational structural design and economical construction, there are lasting needs for a thorough understanding of the adhesion mechanisms to make the enhancement of the performance possible.

There are many literatures that studied the ways of enhancing the strength of placing joint experimentally beginning at very early date [1]. But little study is conducted concerning the relationship between crack path and the performance, which the authors considered to be the most important, constituting the main motivation of this study. The study of crack path should involve the observations of the interface chemically and physically.

The study is effectively executed with employing the latest analyzing equipments such as SEM, EPMA and laser 3-D measuring equipment [2, 3]. The performance of the interface is adequately understood with tension softening diagram (TSD). TSD is the most fundamental feature of fracture mechanics parameters, and the study of it is inevitable for a better understanding of the basic fracture mechanisms. Kurihara [4]

analyzed the TSD of placing joint and led some important aspects of the mechanical properties. The authors have studied TSDs of placing joint and discussed the relationship between strength and ductility of the interface of placing joint with employing models based on TSD [5].

All of the previous studies focus on the individual aspects of the crack path and the mechanical performances with no integrated studies. This paper aims at integrating the knowledge of crack path with the mechanical performances employing the use of the latest analysis equipments and TSD. The evaluated mechanical performances are strength and ductility evaluated in terms of bending strength (fb) and fracture energy (GF) respectively.

## EXPERIMENT AND RESULTS

### *Specimens*

The authors prepared eight types of specimens with a varied type of placing joint made from different roughening or different form on them, and three types of monolithic specimens with a varied size of maximum aggregate for a reference. Table 1 shows the attributes of specimens, and Table 2 the mix proportion of concrete.

The number of specimens was three for each case, which have a section of 100 mm by 100 mm and a length of 400mm. After 24 hours from the 1st cast of concrete in the half part of mold, the joint surface was roughened in the case of R. Then concrete was cast in the remained half of mold as depicted in Figure 1. The specimens were cured in water at 20° C for 28 days after the final cast of concrete. A 50mm depth notch was incised at the center of the specimen before the fracture mechanics test.

Table 1 Attributes of specimens

Specimen	Surface condition	Mold used for placing
N	Monolithic, Max. aggregate size : 20 (mm)	-
N950	WS <sup>*1</sup> , Max. aggregate size : 9.5 (mm)	-
N236	WS <sup>*1</sup> , Max. aggregate size : 2.36 (mm)	-
J	Joint sheet	Joint sheet
E	Exposed aggregate	Non-woven cloth <sup>*2</sup>
R	Roughened with steel wire brush	Steel plate
SP	As-cast	Steel plate
PW	As-cast	Painted ply wood
A	As-cast	Acrylic resin board
G	Sheet glass remained	Sheet glass
FS-3528	Fractured surface	-

\*1: Wet screening was done. \*2: Impregnated with retardant admixture

Table 2 Mix proportion of concrete

W/C (%)	s/a (%)	Weight of materials (kg/m <sup>3</sup> )					Air (%)	Slump (cm)
		Water	Cement	Sand	Gravel	Ad		
51.4	43.0	177	344	739	1010	1.72	3.0	22

Ad: Super plasticizer

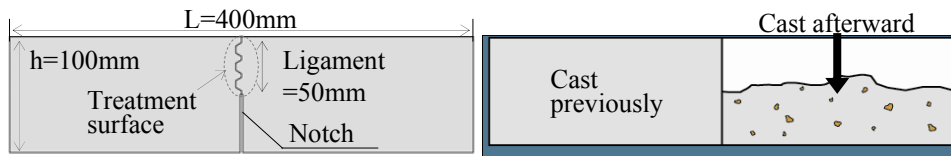


Figure 1 Detail of specimen (left) and method for producing specimen (right)

### ***Fracture mechanics test and analysis***

Fracture toughness test was executed with observing RILEM's recommendation [6]. Load and crack mouth opening displacement (CMOD) were measured continuously during the loading. To cancel the dead weight of specimen and to obtain a good and precise measurement, a counter weight made of steel was glued at each end of specimens. Servo type loading equipment was used to get high-speed response with the help of feed-back system of the equipment.

TSD was achieved from the load-CMOD curve of specimen with employing multi-linear approximation method which was standardized by JCI [7]. Fracture energy is consumed energy during the fracture of a ligament and displayed as an area enclosed with x-axis, y-axis and TSD in the graph, which is abbreviated as GF. The  $f_t$  is tension softening initial stress which is the same as tensile strength, and  $W_{cr}$  is a crack width when load becomes zero (critical crack width).

### ***Resulted Properties***

The authors classified the surface of fractured ligament in two types after fracture mechanics test. One is a fractured part and the other is a detached part. On the basis of eye estimation helped with the results of 3-D laser measuring equipment, the authors refer to whitish and smooth areas as the detached part, and refer to exposed aggregates or rough part, where the height is greater than 0.2mm, as the fractured part.

Table 3 shows the mechanical properties of specimens. The resulted GFs are ranging from 0.002N/mm (specimen G) to 0.05 N/mm (specimen J) with a reference result of 0.1N/mm for specimen N. In Table 3,  $\Phi$  is a ratio of fractured part excluding detached part on the surface divided by the total ligament area. The value  $\Phi$  is different from each other influenced by the conditions of treatment of the joint.  $P_t$  is the maximum height on the fractured surface which was measured with laser 3-D measuring machine.

Table 3 Mechanical properties of specimens

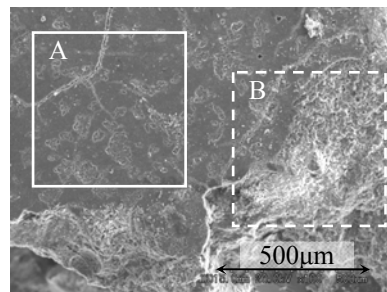
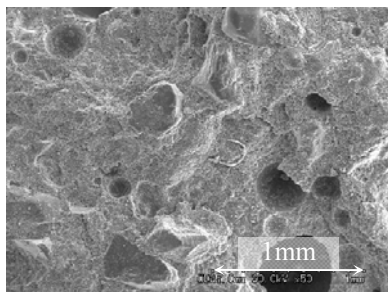
Specimen	fb (MPa)	ft (MPa)	GF (N/mm)	Wcr (mm)	$\Phi$ (-)	Pt (mm)
N-3	4.60	7.28	0.1160	0.2243	1.000	6.47
N950-2	3.66	4.70	0.0642	0.1769	1.000	6.06
N236-2	3.24	3.03	0.0331	0.0400	1.000	4.14
J-3	3.53	4.76	0.0501	0.1174	0.773	5.00
E-3	2.80	3.26	0.0372	0.0835	0.780	5.71
R-2	3.03	5.68	0.0296	0.0507	0.916	2.71
SP-1	2.00	3.65	0.0112	0.0282	0.160	0.96
PW-3	3.28	3.77	0.0543	0.1267	0.816	2.23
A-3	2.51	2.74	0.0148	0.0292	0.369	-
G-2	0.69	1.03	0.0015	0.0119	0.000	0.62
FS-3528-3	2.11	2.11	0.0288	0.1054	0.558	5.99

**Observations by SEM and EPMA**

The authors cut a sample measured 1 cm square from the surface of each specimen. After platinum sputtering on it, surface observations and quantitative analysis of Ca and Si were done with using SEM and EPMA.

Figure 2(a) shows the SEM photo of a sample from specimen-N, where one can observe a rough surface and many fine aggregates half-embedded in it. In the case of specimen-G (Figure 2(b)), one can observe smooth membrane made of  $\text{Ca}(\text{OH})_2$  (area A) and also fractured rough part (area B) where a fine aggregate is projecting. The area B of specimen-G would have contributed to the same strength and GF as the fractured part of specimen-N did, because the appearance of the fractured part is similar.

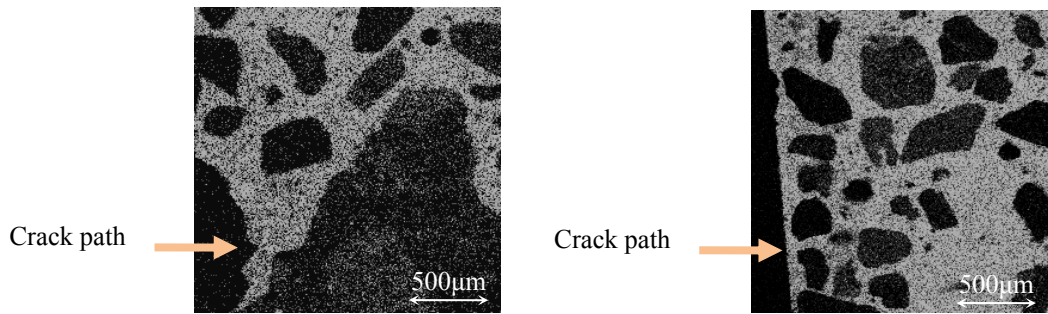
Figure 3(a) and 4(b) are results of quantitative analysis of Ca observed edgewise at the fractured surface (4(a)) and the detached surface (4(b)), telling each crack path. Interfacial transient zone on the surface of aggregate (ITZ) is observed in fractured part of specimen-PW. On the other hand, in Figure 3(b), cement paste which may contain a substantial quantity of  $\text{Ca}(\text{OH})_2$  forms a linear crack path. The thin layer of cement paste isolates linearly distributed fine aggregates, representing the wall effect.



(a) Fractured surface of specimen-N

(b) Detached and fractured surfaces of specimen-G

Figure 2 SEM Observations on the surfaces of specimen-N and -G

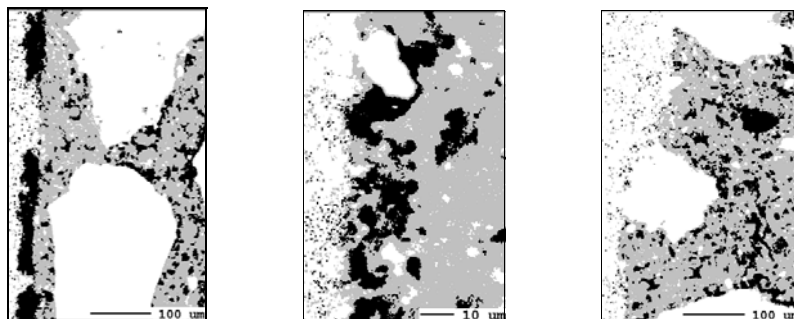


(a) Fractured surface of specimen-PW (b) Detached surface of specimen-A  
Figure 3 Ca detection from the side of the interface by EDX

### PROPOSITION OF CA/SI MAP

As is known, the constituent molar ratio of CaO, SiO<sub>2</sub> and H<sub>2</sub>O in CSH gel is about 3:2:4 and does not have a fixed ratio. If one assumes that a molar ratio of CaO/SiO<sub>2</sub> varies from 1.0 to 2.0, then the mass ratio of Ca/Si varies from 1.43 to 2.85. It means that rough estimation of the mass ratio between 1.0 and 3.0 represents CSH gel. The values over 3.0 represent Ca(OH)<sub>2</sub> and below 1.0 the aggregates or porosity which does not have Ca. The authors elaborated Ca/Si maps which show the mass ratio of Ca divided by Si from the results of quantitative analysis of Ca and Si with EPMA. In the map, gray zones represents CSH gel where the ratio is between 1.0 and 3.0, black zone represents Ca(OH)<sub>2</sub> where the ratio is over 3.0, and white zones represents aggregates mainly consists of SiO<sub>2</sub> or porosity where the ratio is below 1.0.

Figure 4 depicts Ca/Si maps of detached parts of specimen-A, -G and of fractured part of specimen-R. The detached part of specimen-A, -G has thick black layers, meaning that these ones were made of Ca(OH)<sub>2</sub>. Fractured surface of specimen-R has no such black layer, though Ca/Si is high around some aggregates in Figure 4(c). Almost all of the parts can be assumed to be CSH gel, because the gray zone is abundant telling the effects of roughing. It can be said that the Ca/Si map revealed the weak layer of Ca(OH)<sub>2</sub> which plays a primary role on the crack path.



(a) specimen-A (b) specimen-G (c) specimen-R  
Figure 4 Ca/Si maps observed from the side of the interface

## DISCUSSION

### What $\Phi$ determines

Figure 5 shows a relationship between ft ratio and  $\Phi$ , which tells that ft ratio depends on  $\Phi$ , and the dependence is influenced by the size of aggregate. So, three lines can be drawn from specimen-G to specimen-N, -N950 or -N236. Figure 5 also tells that the layer mostly made of  $\text{Ca}(\text{OH})_2$  on the surface of specimen-G (Fig. 4) contributed to ft as about 20 % as the specimen-N did. This value of ft is caused by a chemical adhesion between sheet glass and a layer of  $\text{Ca}(\text{OH})_2$ .

A relationship between Pt and  $\Phi$  is depicted in Figure 6, which indicates that  $\Phi$  is strongly related to Pt. But the dependence on the size of aggregate is not clear. Then it can be said that the ft and Pt are mainly determined by  $\Phi$ .

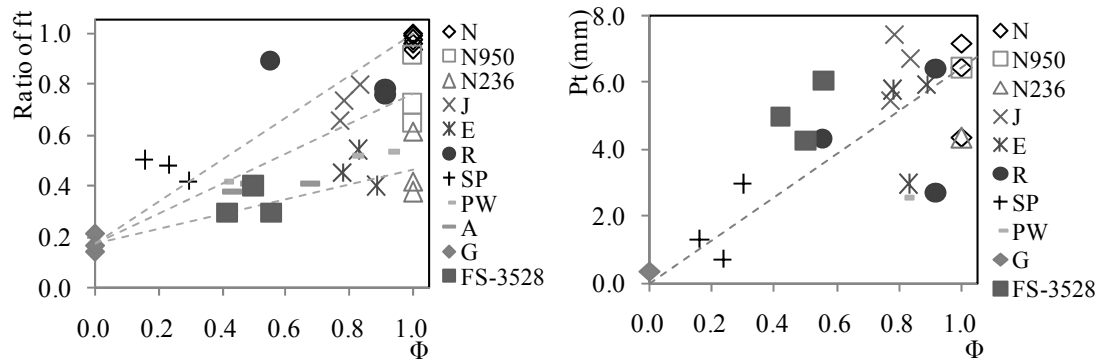
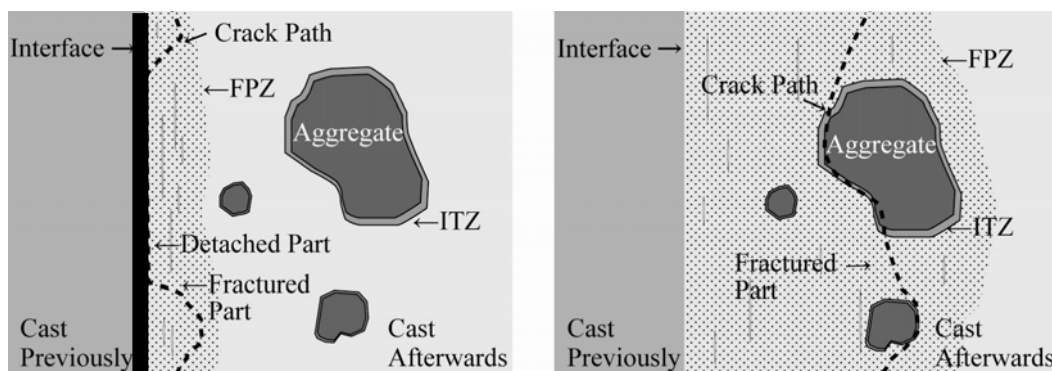


Figure 5 Relationship between ft ratio and  $\Phi$  Figure 6 Relationship between Pt and  $\Phi$

### FPZ and Crack Path

Figure 7 represents models of crack paths of interfacial surfaces which have different interfacial strengths. The crack path of weak interface whose chemical adhesion is deteriorated by  $\text{Ca}(\text{OH})_2$  makes mostly the linear crack path as is depicted in Figure 7(a).



(a) Crack path of weak interface (b) Crack path of strong interface  
Figure 7 Crack path affected by strength of interface

On the other hand, Figure 7(b) shows the crack path of strong interface, where the path passes around ITZ which is a weak layer made of  $\text{Ca}(\text{OH})_2$ , constituting rough and wide area of fractured part. At the same time, these interfacial strengths determine the ranges of fracture process zone (FPZ) which is related to the Pt. Then, it is important to know that  $\Phi$  is a resulted value which represents the strength of the interface (related to ft) and the range of FPZ (related to Pt).

If the Pt works as a dowel against pull-out load, the Pt should be relational to Wcr (critical width). Figure 8 shows a relationship between Pt and Wcr. There is the same relationship between Pt and Wcr as is shown in Figure 5 which depicts ft ratio and  $\Phi$ .

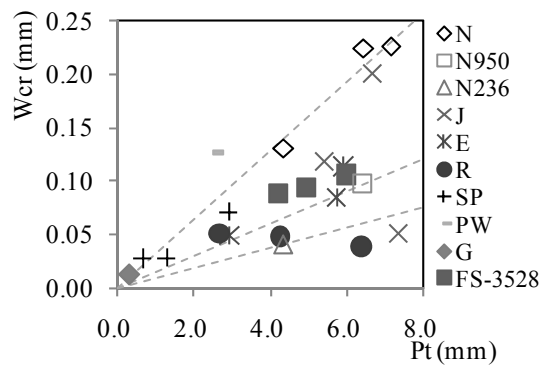


Figure 8 Relationship between Pt and Wcr

#### ***Relationship between Mechanical Performance and $\Phi$***

Figure 9 shows a relationship between normalized GF and  $\Phi$ , which is similar to Figure 8. Normalized GF and  $\Phi$  have a strong relation because GF is dependent to Wcr, and Wcr is dependent to Pt (Fig. 8), and also Pt is dependent to  $\Phi$  (Fig. 6).

From Figure 10, it is observed that normalized fb and  $\Phi$  have a strong relation with a small influence by the size of aggregate. The relation derives from the fact that ft ratio and  $\Phi$  have a relation (Fig. 5) whereas ft is related to fb as is well known.

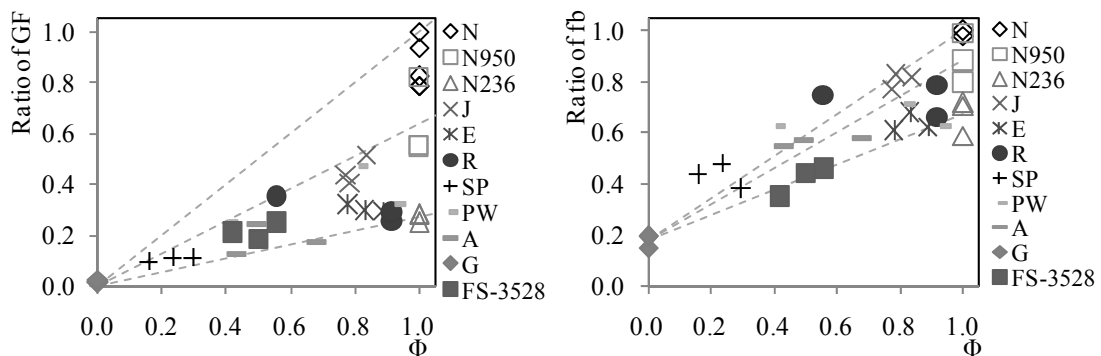


Figure 9 Relationship between GF ratio and  $\Phi$  Figure 10 Relationship between fb ratio and  $\Phi$

In summary, the total relationship can be depicted as is shown in Figure 11. The important point is that the crack path is quantitatively evaluated by the two values;  $\Phi$  and  $P_t$ . These two values are essential to two mechanical performances; strength ( $f_b$ ) and ductility (GF).

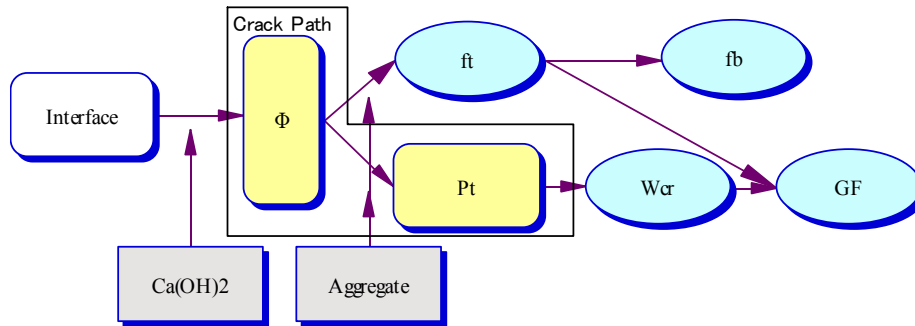


Figure 11 Relationship between crack path and mechanical properties of interface

## CONCLUSIONS

The authors conducted fracture mechanics test of eight different types of concrete prisms which have a vertical placing joint, and three types of monolithic ones which have different size of aggregate. The findings are as follows.

- [1] Crack path is specific for each specimen with no common similarity but it can be quantitatively evaluated by two values;  $\Phi$  and  $P_t$ .
- [2] The strength ( $f_b$ ) of the interface is dependent to  $\Phi$ , and also ductility (GF) is dependent to  $\Phi$ .
- [3] As both  $f_t$  and  $P_t$  are influenced by the size of aggregate, both strength and GF are affected by it.
- [4] The most important treatment for the better mechanical performance for the interface is removing  $\text{Ca(OH)}_2$  and obtain large  $\Phi$ .

## REFERENCES

1. Kokubu, M. (1950) *Trans. JSCE*, **8**, 1-24, JSCE, Tokyo.
2. Satoh, A., Yamada, K. and Ishiyama, S. (2007) *Proc. AIJ Tohoku chap.*, **70**, 49-55.
3. Satoh, A., Yamada, K. and Ishiyama, S. (2008) *Proc. AIJ Tohoku chap.*, **71**, 1-8.
4. Kurihara, T., Ando, T., Uchida, Y. and Rokugo, K. (1996) *Proc. ann. meet. JCI*, **18(2)**, 461-466.
5. Satoh, A., Yamada, K., and Ishiyama, S.(2008) *Proc. 17 Eur. Conf. Frac.*, 1530-1537.
6. RILEM Draft Recommendation (1985) *Mat. Str.*, **18(106)**, 285-290.
7. Izumi, I. (ed.) (2004) *JCI standards*, JCI, Tokyo.